

# Expectations vs. Realities: The Cost of MSE-Optimal Forecasting Under Conditional Uncertainty

Riku Green  
riku.green@bristol.ac.uk  
The University of Bristol  
Bristol, UK

Zahraa S. Abdallah  
zahraa.abdallah@bristol.ac.uk  
The University of Bristol  
Bristol, UK

Telmo M Silva Filho  
telmo.silvafilho@bristol.ac.uk  
The University of Bristol  
Bristol, UK

## Abstract

Multi-step time series forecasting (MSF) is commonly evaluated using point-wise error metrics such as mean squared error (MSE), implicitly treating the conditional mean as a sufficient target. We show that this can be misleading under conditional uncertainty, where the conditional expectation becomes unrepresentative of typical realized values at longer horizons. We formalize this effect through a conditional uncertainty gap and prove that whenever this gap is nonzero, no deterministic predictor can simultaneously minimize MSE and match the marginal distribution of realized futures. This establishes a fundamental, model-agnostic trade-off between point accuracy and marginal realism in MSF evaluation. Using controlled stochastic dynamical systems and nine real-world forecasting benchmarks, we empirically characterize the resulting accuracy–realism frontier and **quantify the practical cost of MSE-only model selection**. As conditional uncertainty increases with forecast horizon, the attainable set expands into a pronounced Pareto front, separating MSE-optimal but under-dispersed predictors from methods that trade accuracy for realistic *marginal variability*. **Across benchmarks, we find that small relaxations in MSE ( $\leq 5\%$ ) frequently unlock disproportionate gains in marginal realism, with median improvements of 17.3% and gains exceeding 30% in some datasets.** We further show that common forecasting strategies systematically occupy different regions of this frontier: direct multi-output predictors concentrate near the accuracy-optimal extreme, while recursive strategies and sample-based inference favors marginal realism. Together, these results expose a structural failure mode of MSE-based evaluation in long-horizon forecasting and recast strategy and inference selection as navigation of an unavoidable accuracy–realism trade-off.

## CCS Concepts

• **Computing methodologies** → **Machine learning**.

## Keywords

Time series forecasting, multi-step prediction, conditional uncertainty, evaluation metrics, data mining

## ACM Reference Format:

Riku Green, Zahraa S. Abdallah, and Telmo M Silva Filho. 2026. Expectations vs. Realities: The Cost of MSE-Optimal Forecasting Under Conditional Uncertainty. In *Proceedings of the 32nd ACM SIGKDD Conference*



This work is licensed under a Creative Commons Attribution 4.0 International License. *KDD '26, Jeju Island, Republic of Korea*  
© 2026 Copyright held by the owner/author(s).  
ACM ISBN 979-8-4007-2259-2/2026/08  
<https://doi.org/10.1145/3770855.3818087>

on *Knowledge Discovery and Data Mining V.2 (KDD '26)*, August 09–13, 2026, Jeju Island, Republic of Korea. ACM, New York, NY, USA, 12 pages.  
<https://doi.org/10.1145/3770855.3818087>

## 1 Introduction

Multi-step time series forecasting (MSF) is a fundamental problem in machine learning and statistics, with applications in domains such as energy systems, finance, traffic prediction, and climate modeling [12]. Given a window of past observations, the task is to predict a sequence of future values over a fixed horizon. Recent benchmarking typically assesses performance using point-wise error metrics such as mean squared error (MSE) [9, 10, 14, 20, 25, 31], implicitly treating the conditional expectation of the future as the desired prediction target.

However, this assumption becomes fragile as the forecast horizon increases. In many real-world systems, uncertainty accumulates over time [2], and the conditional distribution of future outcomes given the past becomes increasingly dispersed. This occurs whenever realizations diverge in qualitatively different ways from the same initial condition, as illustrated in Figure 1a. As the horizon grows, the expectation–realization gap widens (Figures 1b and 1c), and the conditional expectation—the target induced by MSE—need not correspond to a typical realized outcome [13]. Empirical benchmark studies [32] confirm this effect: MSE-optimized forecasts often become increasingly under-dispersed at long horizons. This suggests a tension between forecasting conditional expectations and producing forecasts that are distributionally representative of realized futures.

To formalize this effect, we introduce a conditional uncertainty gap that measures the fraction of future variability that is irreducible given the past. When this gap is nonzero, the conditional expectation becomes unrepresentative of typical realizations. We show that in such regimes, no deterministic predictor can simultaneously minimize mean squared error and match the *marginal* distribution of true future values (across instances at horizon  $h$ ). In other words, pointwise accuracy and marginal realism become fundamentally incompatible objectives. This induces an unavoidable Pareto trade-off [18] between approximating conditional expectations and reproducing the distribution of realized futures. Crucially, this trade-off is independent of model class, training procedure, or architectural choice: it is a structural property of multi-step prediction under conditional uncertainty. As a consequence, evaluation protocols that select models solely by MSE can systematically favor under-dispersed forecasts, even when alternatives with nearly identical error better match the distribution of realized futures.

This perspective reveals that common forecasting strategies implicitly select different operating points on this trade-off. Direct

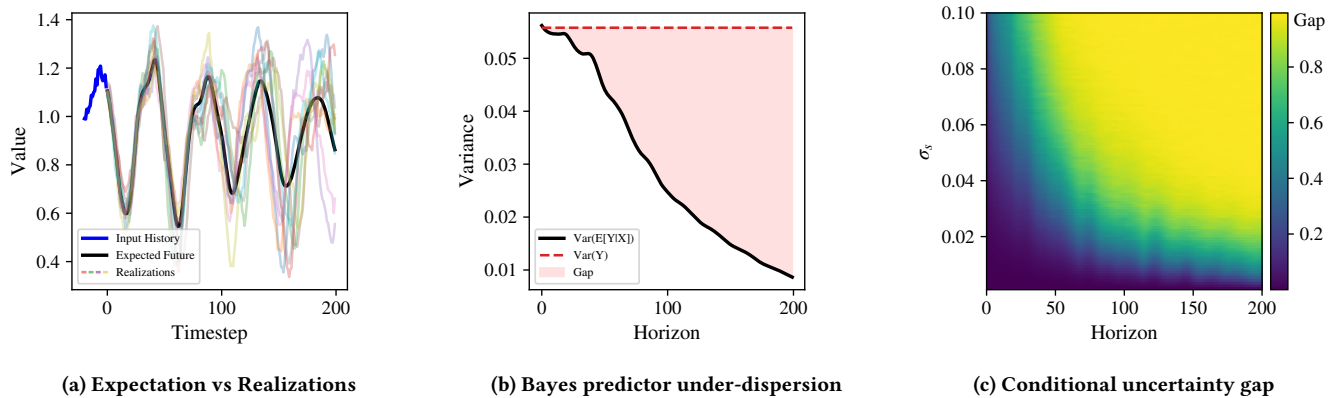


**Figure 1: Visualizing the forecasting gap.** (a): As the horizon increases, realized trajectories (colored) diverge from the smooth conditional expectation (black), motivating how the “average” future can become unrepresentative of typical realized outcomes. (b): The MSE-optimal predictions computed over multiple instances fail to match the target’s marginal variability across instances: the predictive marginal variance (black) drops below the true marginal variance (red dashed), yielding a widening variance gap. (c): Increasing stochasticity ( $\sigma_s$ ) induces larger conditional uncertainty, and the gap grows with horizon.

multi-output predictors, aligned with estimating conditional expectations under squared loss [28], concentrate near the MSE-optimal extreme and often produce smoothed, under-dispersed forecasts. Recursive strategies, by contrast, propagate variability through time and therefore *can* generate trajectories that more closely resemble typical realizations, but at the cost of higher pointwise error. Probabilistic forecasting models do not remove this tension: different inference rules (e.g., predictive mean or single-sample rollout) simply occupy different regions of the same accuracy–realism frontier.

Our findings support the view that multi-step forecasting cannot be fully characterized by pointwise error alone [32]. Squared loss elicits the conditional mean, but under conditional uncertainty this functional can become unrepresentative of typical realized futures. This helps explain why recursive, direct, and probabilistic inference rules often dominate in different regimes [7, 9, 28]: each strategy prioritizes a different functional of the future distribution, and whether these priorities align depends on the underlying data-generating process. When the conditional uncertainty gap is small, MSE-optimality and realism are largely aligned; as the gap grows, they separate into an accuracy–realism frontier. Across real-world benchmarks, a modest 5% increase in MSE frequently yields large gains in marginal realism, with a median improvement of 17%.

Our goal is not to propose a new forecasting architecture, but to turn this trade-off into a practical model-selection protocol. We recommend keeping MSE as the primary constraint, then using inexpensive distributional diagnostics such as marginal  $W_1$  to choose among near-MSE-optimal candidates.

Our contributions are threefold:

- **A theoretical explanation of over-smoothing in long-horizon forecasting.** We prove that no deterministic predictor can minimize mean squared error and match the distribution of realized futures. This explains a common long-horizon failure mode: MSE-optimal predictors are necessarily under-dispersed, not because of model misspecification but due to irreducible conditional uncertainty.

- **Quantifying the practical accuracy–realism trade-off.**

We empirically characterize the resulting accuracy–realism Pareto frontier and show that it is readily attainable in practice. Across synthetic systems and real-world benchmarks, small relaxations in MSE often yield disproportionately large gains in marginal realism, demonstrating that strict MSE-based model selection can incur substantial and avoidable realism costs.

- **Forecasting strategy as a practical control knob.** While probabilistic sampling naturally navigates the accuracy–realism trade-off, we show empirically that the *multi-step strategy* itself (direct versus recursive prediction) provides a simple and effective mechanism for moving along the Pareto frontier. This reframes strategy selection as a concrete design choice for trading pointwise error against distributional representativeness, independent of model class.

## 2 Conditional Uncertainty in MSF

This section formalizes how uncertainty accumulates in multi-step forecasting and why the conditional mean can cease to be representative of *realized* futures. We aim to characterize intrinsic uncertainty in  $Y_h | X$  before our main accuracy–realism result.

*Multi-Step Forecasting Setup.* Let  $\{y_t\}_{t \in \mathbb{Z}}$  be a real-valued stochastic time series with bounded second moments,

$$\sup_t |y_t| < \infty, \quad \text{Var}(y_t) < \infty. \quad (1)$$

For simplicity, we assume weak stationarity so that  $\mathbb{E}[y_t]$  and  $\text{Var}(y_t)$  are time-invariant. Given a window length  $L$ , define the past context and the  $h$ -step-ahead target as

$$\mathbf{X} = (y_{t-L}, \dots, y_{t-1}) \in \mathbb{R}^L, \quad Y_h = y_{t+h}. \quad (2)$$

Multi-step forecasting seeks a predictor  $f_h : \mathbb{R}^L \rightarrow \mathbb{R}$  such that  $f_h(\mathbf{X})$  approximates  $Y_h$ .

For a fixed horizon  $h$ ,  $Y_h$  is a random variable conditional on the past  $\mathbf{X}$ . By the law of total variance,

$$\text{Var}(Y_h) = \text{Var}(\mathbb{E}[Y_h | \mathbf{X}]) + \mathbb{E}[\text{Var}(Y_h | \mathbf{X})]. \quad (3)$$

The first term,  $\text{Var}(\mathbb{E}[Y_h | \mathbf{X}])$ , quantifies how much the conditional mean varies across different pasts. The  $\mathbb{E}[\text{Var}(Y_h | \mathbf{X})]$  term measures the average spread of future outcomes given the same past. As the forecast horizon  $h$  increases,  $\mathbb{E}[\text{Var}(Y_h | \mathbf{X})]$  typically increases due to noise [28]. This can occur when the unconditional variance of  $Y_h$  remains bounded, reflecting the accumulation of uncertainty over time.

We define a horizon-dependent signal-to-noise ratio

$$\text{SNR}_h = \frac{\text{Var}(\mathbb{E}[Y_h | \mathbf{X}])}{\text{Var}(\mathbb{E}[Y_h | \mathbf{X}]) + \mathbb{E}[\text{Var}(Y_h | \mathbf{X})]}. \quad (4)$$

This quantity measures the fraction of total variability explained by systematic dependence on the past.

Equivalently, we define the *conditional uncertainty gap*

$$\text{Gap}_h = 1 - \text{SNR}_h = \frac{\mathbb{E}[\text{Var}(Y_h | \mathbf{X})]}{\text{Var}(\mathbb{E}[Y_h | \mathbf{X}]) + \mathbb{E}[\text{Var}(Y_h | \mathbf{X})]}. \quad (5)$$

When  $\text{Gap}_h$  is small, realized values at horizon  $h$  are tightly concentrated around  $\mathbb{E}[Y_h | \mathbf{X}]$ , so the conditional mean is representative. When  $\text{Gap}_h$  is large, irreducible uncertainty dominates:  $\mathbb{E}[Y_h | \mathbf{X}]$  explains little of the variance of realized  $Y_h$ , and even a perfect estimator of the conditional mean can yield forecasts that under-represent the marginal variability of realized futures.

### 3 Evaluation-Induced Accuracy–Realism Trade-offs

MSF evaluation practice primarily treats the conditional mean as the sole prediction target and underlies much of the empirical comparisons made in the literature [9, 10, 14, 31]. At the same time, empirical studies have repeatedly observed that MSE-optimal forecasts can appear overly smooth or unrepresentative of typical realized futures, particularly at longer horizons [13].

In this section, we show that this phenomenon is not an artifact of model capacity, optimization, or forecasting strategy, but instead reflects a structural limitation of *standard multi-step forecasting evaluation*. Our goal is to *formalize when and why commonly used evaluation objectives implicitly force a trade-off* between pointwise accuracy and distributional realism. We focus on deterministic point forecasters and compare pointwise accuracy, measured by MSE, to *marginal* distributional realism measured by the Wasserstein distance  $W_1$  [27]. This choice reflects both the structure of standard evaluation protocols and the mechanism underlying over-smoothing.

Under typical MSF evaluation, each input context  $\mathbf{X}$  is associated with a single realized future  $Y_h$ , and each deterministic forecaster produces a single prediction  $f_h(\mathbf{X})$ . As a result, the conditional distribution  $p(Y_h | \mathbf{X})$  is not directly observable, and proper scoring rules such as CRPS [6, 11] cannot be applied to deterministic forecasts. The only distributional information consistently identifiable from standard evaluation data is the *marginal distribution across contexts*, obtained from the samples  $\{f_h(\mathbf{X}_i)\}_{i=1}^N$  and  $\{Y_{h,i}\}_{i=1}^N$ . For this reason, marginal distribution matching represents the *weakest nontrivial notion of realism* that can be evaluated under standard

deterministic MSF protocols. Importantly, it is also directly aligned with the mechanism behind over-smoothing: the collapse of marginal variance induced by MSE-optimal predictors.

We emphasize that marginal realism does not guarantee full trajectory realism. However, failure at the marginal level necessarily implies failure under any stronger notion of realism. Since any trajectory-level or conditional distributional match implies equality of the corresponding horizon-wise marginals by projection, failure to match the marginal distribution at any horizon precludes these stronger notions of realism (Appendix C). We further show that analogous incompatibilities arise at the trajectory level and for stochastic predictors under squared loss. Thus, the phenomenon is not specific to marginal  $W_1$  nor to deterministic forecasting.

*Setup.* Let  $\mathcal{L}(Z)$  denote the (marginal) law of a random variable  $Z$ . Let  $f_h(\mathbf{X})$  be any deterministic predictor of the future value  $Y_h$  given the past  $\mathbf{X}$ . We evaluate such predictors using two criteria:

- (1) **Pointwise accuracy**, measured by mean squared error,

$$\mathcal{R}_{\text{MSE}}(f_h) = \mathbb{E}[(f_h(\mathbf{X}) - Y_h)^2]. \quad (6)$$

- (2) **Distributional realism**, measured by agreement between the marginal laws  $\mathcal{L}(f_h(\mathbf{X}))$  and  $\mathcal{L}(Y_h)$ .

Under squared loss, the first criterion is uniquely minimized by the conditional expectation  $f_h^*(\mathbf{X}) = \mathbb{E}[Y_h | \mathbf{X}]$ . The second criterion requires that the marginal distribution of predictions match that of realized futures. Standard evaluation therefore implicitly asks for both properties simultaneously. The following theorem shows that, whenever conditional uncertainty is non-degenerate, this objective is internally inconsistent.

**THEOREM 1 (ACCURACY–REALISM TRADE-OFF).** *Assume  $\text{Var}(Y_h) \in (0, \infty)$  and  $\text{Gap}_h > 0$ . Then no deterministic predictor  $f_h$  can simultaneously*

- (1) *minimize mean squared error,*
- (2) *and match the marginal distribution of  $Y_h$ .*

*More precisely, if  $f_h^*(\mathbf{X}) = \mathbb{E}[Y_h | \mathbf{X}]$  denotes the MSE-optimal predictor, then*

$$W_1(\mathcal{L}(f_h^*(\mathbf{X})), \mathcal{L}(Y_h)) > 0. \quad (7)$$

*Conversely, any deterministic predictor whose marginal distribution satisfies  $\mathcal{L}(f_h(\mathbf{X})) = \mathcal{L}(Y_h)$  must incur strictly larger mean squared error than  $f_h^*$ .*

**PROOF SKETCH.** Under squared loss, the unique minimizer of pointwise risk is the conditional expectation  $f_h^*(\mathbf{X}) = \mathbb{E}[Y_h | \mathbf{X}]$ . By the law of total variance,

$$\text{Var}(Y_h) = \text{Var}(\mathbb{E}[Y_h | \mathbf{X}]) + \mathbb{E}[\text{Var}(Y_h | \mathbf{X})].$$

When  $\text{Gap}_h > 0$ , the second term is strictly positive, implying that  $\text{Var}(f_h^*(\mathbf{X})) < \text{Var}(Y_h)$ . Since the two variables share the same mean, their marginal distributions cannot coincide. For one-dimensional distributions with finite second moments, this variance mismatch implies a strictly positive  $W_1$  distance. The converse follows because any predictor matching the marginal distribution of  $Y_h$  must have variance  $\text{Var}(Y_h)$  and therefore cannot coincide almost surely with  $f_h^*(\mathbf{X})$ , implying strictly larger MSE.  $\square$

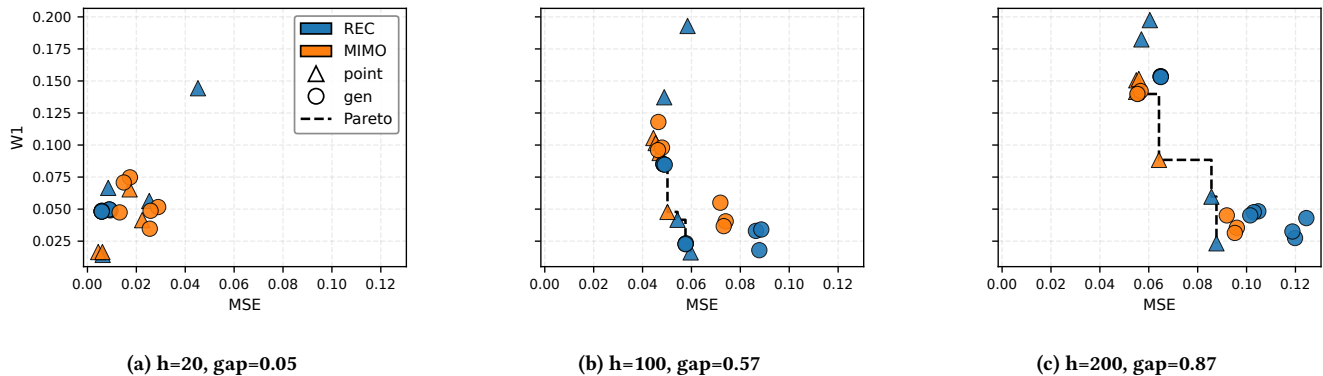


Figure 2: Attainable accuracy–realism trade-offs under low and high conditional uncertainty. MSE versus marginal  $W_1$  distance for a representative low-gap regime (left) and high-gap regime (right) in the stochastic Mackey–Glass [16] system. Each point corresponds to a trained forecasting strategy. When the gap is small, methods cluster near a single operating point. As the gap increases, the attained set of performances expands into a clear Pareto frontier, separating MSE-optimal but under-dispersed predictors from methods that trade accuracy for improved marginal realism.

### 3.1 Implications for Forecasting Objectives

**The trade-off is induced by evaluation, not by the learning algorithm.** When  $\text{Gap}_h > 0$ , Theorem 1 shows that no deterministic forecaster can be both MSE-optimal and marginally realistic under standard evaluation. This under-dispersion of the conditional mean is therefore not a consequence of limited model capacity, suboptimal optimization, or the choice of multi-step forecasting strategy, but instead reflects the conditional distribution of  $Y_h$  itself.

**Forecast evaluation implicitly selects an operating point.** Deterministic forecasters therefore lie on an intrinsic accuracy–realism Pareto frontier. The conditional expectation occupies the MSE-optimal extreme, while moving toward marginal realism necessarily incurs additional pointwise error. This explains why empirical comparisons that rank models solely by MSE may systematically favor oversmoothed forecasts. Learning a predictive distribution does not eliminate this tension: deployed forecasts still arise from a deterministic decision rule (e.g., using the mean versus sampling), which selects an operating point on the same frontier. In Section 4, we show empirically that this trade-off arises in practice and grows with the conditional uncertainty gap, and that trajectory-level realism metrics exhibit the same qualitative frontier structure.

## 4 Empirical Characterization of the Trade-off

Given the intrinsic frontier implied by Section 3, our goal is to characterize its empirical manifestation and quantify the practical cost of MSE-only evaluation. Our empirical results support three claims: (i) the attainable accuracy–realism frontier expands with conditional uncertainty; (ii) small relaxations in MSE frequently unlock disproportionate gains in realism; and (iii) forecasting strategies and inference rules systematically populate different regions of this frontier. The remainder of this section supports these claims in controlled systems and real-world benchmarks.

We measure marginal realism using  $W_1$  distance, which directly aligns with Theorem 1. To ensure conclusions are not specific to a

single notion of realism, we also report trajectory-level and multivariate realism metrics. Dynamic Time Warping (DTW), Vector Wasserstein ( $W_{1-vec}$ ), order-preserving Wasserstein (OPW), and fused Gromov–Wasserstein (FGW)); additional robustness are provided in Appendices B and B.4. These serve as robustness checks; our main empirical claims are stated in terms of marginal  $W_1$ , which is the weakest distributional notion identifiable under standard deterministic MSF evaluation.

Across datasets, we evaluate the same base predictors under recursive (REC) and direct multi-output (MIMO) strategies. Our deterministic predictors include Linear Ridge Regression (LR), Multilayer Perceptrons (MLP), and Decision Trees (DT). We prioritize empirical coverage over state-of-the-art accuracy. To confirm the incompatibility is model-agnostic, we replicate results for Chronos [1] in Appendix B.5. We additionally train conditional normalizing flows [4] and evaluate them via deterministic decision rules (e.g., predictive mean and single-sample rollouts), allowing us to compare how probabilistic models *navigate* the attainable trade-offs through inference choice. Implementation details and hyperparameters are deferred to Appendix A. For each horizon  $h \in [1, \dots, 200]$ , each trained method induces a point in objective space ( $\text{MSE}_h, W_{1h}$ ) (lower is better on both axes). We summarize the best achievable compromises by the empirical Pareto front over the evaluated methods.

### 4.1 Controlled Trade-off Geometry

We begin with a controlled synthetic system in which conditional uncertainty can be directly measured. This allows us to relate the geometry of the attainable accuracy–realism frontier to the conditional uncertainty gap defined in Section 3.

We generate time series from a stochastic Mackey–Glass system [16] with additive state noise of magnitude  $\sigma_s$ . Varying  $\sigma_s$  continuously controls the level of conditional uncertainty while keeping the dynamics bounded.

For each evaluation context  $\mathbf{x}_i$ , we approximate the conditional distribution  $p(Y_h | \mathbf{X} = \mathbf{x}_i)$  using  $M = 1000$  independent stochastic

rollouts. This enables direct estimation of the conditional uncertainty gap  $\text{Gap}_h$  as well as the evaluation objectives  $\text{MSE}_h$  and  $W_{1h}$ . Full simulation details are provided in Appendix A.3.

Figure 1 shows that  $\text{Gap}_h$  increases monotonically with both forecast horizon  $h$  and noise level  $\sigma_s$ . The system therefore spans regimes ranging from low conditional uncertainty, where the conditional expectation is representative of typical futures, to high uncertainty, where it is not. This controlled setting matches the assumptions of the theoretical analysis and provides a reference for interpreting the geometry of empirical trade-offs.

**Pareto Geometry Under Low and High Gap.** We explore how the accuracy–realism trade-off from Theorem 1 appears in practice. We focus on the geometry of the *attainable* trade-offs induced by a finite set of trained models.

In low-gap regimes (Figure 2a), methods cluster tightly in objective space. Here, minimizing MSE also yields low  $W_1$  discrepancy, indicating that the conditional expectation remains representative of marginal outcomes and the attainable frontier is effectively degenerate.

As  $\text{Gap}_h$  increases, the attainable set expands into a clear Pareto frontier. Methods separate along the accuracy–realism axis: some concentrate near the MSE-optimal extreme by collapsing toward the conditional expectation, while others trade pointwise accuracy for improved marginal realism. This separation reflects the incompatibility identified in Theorem 1 and shows how it materializes under different forecasting approaches.

**Trade-off geometry grows with conditional uncertainty.** To summarize the size of the attainable accuracy–realism trade-off, we measure the length of the Pareto front induced by the trained forecasters. Longer fronts indicate a wider set of non-dominated operating points. Figure 3 shows that Pareto front length increases monotonically with the estimated gap  $\text{Gap}_h$  across all realism metrics, indicating an expanding attainable trade-off as conditional uncertainty grows.

### 4.2 Local Cost of Prioritizing MSE

The Pareto front characterizes the full set of attainable accuracy–realism trade-offs, but standard evaluation protocols typically operate near the MSE-optimal extreme [9, 14, 25]. We therefore analyze the *local* behavior of the frontier to quantify how often a small relaxation in MSE yields a net-positive realism trade.

For each noise level and forecast horizon, we extract the Pareto front in the  $(\text{MSE}, W_1)$  plane and consider the first two Pareto-optimal models ordered by increasing MSE. Let  $\Delta_{\text{MSE}}$  denote the relative MSE increase required to move from the MSE-optimal model to the next Pareto-optimal alternative, and let  $\Delta_{W_1}$  denote the corresponding relative reduction in marginal  $W_1$ . We call this step a *successful trade* when  $\Delta_{W_1} > \Delta_{\text{MSE}}$ .

Figure 4 reports that successful trades are prevalent across essentially all gap values (global average 84.1%), indicating that even small relaxations in MSE frequently deliver larger relative improvements in marginal realism.

### 4.3 Frontier Navigation via MSF Strategies

Having characterized the attainable accuracy–realism frontier, we now illustrate how common forecasting strategies *navigate* this

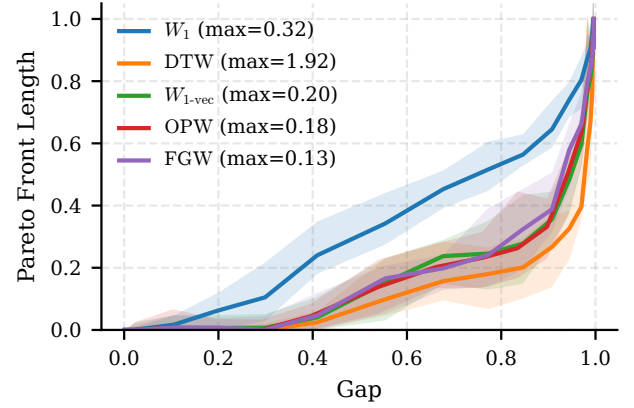


**Figure 3: Pareto front length as a function of the estimated conditional uncertainty gap for different realism metrics. For comparability, front lengths are normalized by the maximum raw length attained by each metric (reported in the legend). Curves show median values within quantile bins of Gap, with shaded regions indicating interquartile ranges. All metrics exhibit a monotonic increase in attainable trade-off size with gap, indicating that higher conditional uncertainty induces a wider accuracy–realism frontier.**

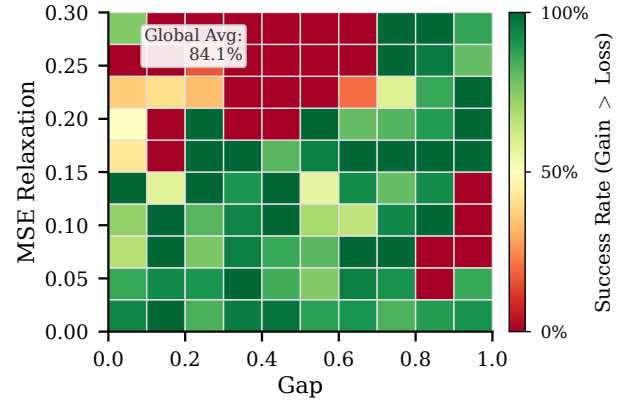


**Figure 4: Local trade-offs between MSE relaxation and realism gain when moving from the top two MSE-optimal models in the Pareto front under  $W_1$  metric on MG experiments. The percentage where relative realism gains ( $W_1$ ) were greater than its MSE relaxation, binned by Gap ( $x$ -axis) and MSE relaxation ( $y$ -axis). Colors show the percentage of trials where Gain > Loss. Wider gaps offer wider relaxation success rates.**

space. Figure 2 shows that direct (MIMO) and recursive (REC) strategies consistently occupy different regions of the frontier, particularly in high-gap regimes. Direct strategies cluster near the MSE-optimal extreme, while recursive strategies more frequently trade accuracy for improved marginal realism.

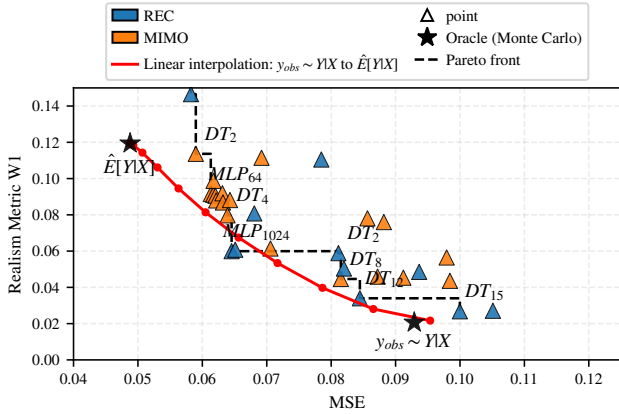


**Figure 5: Inference rules navigate the accuracy–realism Pareto frontier.** Oracle prediction performance (stars) obtained via MC rollouts from the true conditional distribution shown as the expected future (mean  $\mathbb{E}[Y | X]$ ) and single-sample inference ( $Y \sim p(Y | X)$ ). Linear interpolation (red line) shows that inference rules select operating points along the intrinsic (MSE,  $W_1$ ) frontier even in the absence of epistemic error. Recursive (REC) and direct multi-output (MIMO) point strategies shown in blue and orange respectively. MLP width and decision tree depth indicated by subscripts.

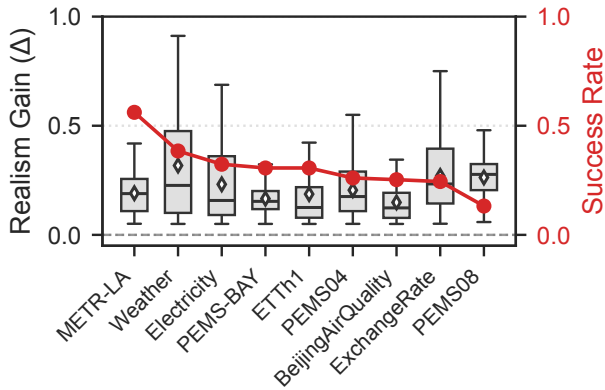


**Figure 6: Real-world accuracy–realism trade-offs under a 5% MSE tolerance.** Boxplots show the distribution of relative marginal realism gains ( $W_1$ ) attainable by Pareto-optimal alternatives whose MSE is within 5% of the MSE-optimal model for each dataset. Red markers indicate the success rate: the fraction of cases in which the realism gain exceeds the corresponding MSE loss. Results highlight substantial attainable realism improvements in several datasets, alongside marked heterogeneity across domains.

Using the same high-gap regime, in Figure 5 we further isolate the role of inference using oracle access to the conditional distribution, thereby eliminating modeling and optimization error. Different

summaries of the same predictive distribution induce distinct operating points: mean inference concentrates near the MSE-optimal extreme, while single-sample inference trades pointwise accuracy for improved marginal realism. This shows that probabilistic forecasting navigates, rather than resolves, the intrinsic accuracy–realism tension. Linear interpolation between these summaries traces a continuous path along the frontier. The same ‘inference-as-control’ effect appears when we used a zero-shot Chronos Time Series Foundation Model [1] on real world datasets in Appendix B.5. Theorem 1 and Appendix C support these empirical results.

#### 4.4 Opportunity Cost of MSE-Only Model Selection on Real Benchmarks

We evaluate 9 real-world forecasting benchmarks from [25], spanning energy demand, traffic, weather, air quality, and finance. For each dataset, we treat the first 7 variates as independent univariate series and evaluate a forecast horizon of 200 steps. This yields  $9 \times 7 \times 200 = 12,600$  horizon-specific evaluations (Pareto fronts). Dataset details appear in Appendix A.

**Price of “MSE-only” evaluations.** To quantify the practical cost of strict MSE-based selection, we fix a tolerance  $\epsilon = 5\%$  around the MSE-optimal model. For each horizon, we identify near-ties whose MSE lies within  $(1 + \epsilon)\%$  of the optimum and record the best attainable improvement in marginal realism. We call this a *successful opportunity* when the realism gain exceeds the MSE loss (i.e.,  $\Delta\text{Realism} > \Delta\text{MSE}$ ). This yields, for each dataset, a distribution of attainable realism improvements and a success probability.

Figure 6 reports these quantities across datasets. Across all nine datasets, under a 5% MSE tolerance, the median attainable marginal realism improvement is **17.3%**, with a median success probability of **30.6%**. This shows that strict MSE-only selection can systematically discard substantially more realistic forecasts, even when accuracy differences are small. At the dataset level, the effect is often larger. For example, **Weather** admits a median realism improvement of **22.6%** with success probability **38.4%**, and **ExchangeRate** admits **23.3%** with success probability **24.4%**. Even when success is less frequent, unrealized gains can remain large: **PEMS08** admits **27.7%** median improvement but succeeds in **13.2%** of cases. As a robustness check, we reproduce the same  $\epsilon = 5\%$ -opportunity analysis using zero-shot Chronos-T5 and observe consistent positive median realism gains with high success rates in Appendix B.5.

**Benchmark-wide pattern and robustness.** The opportunity cost varies across benchmarks, reflecting differences in conditional uncertainty, model misspecification, and data regime. However, the effect is not a corner case: every dataset contains cases where near-MSE-optimal models offer materially better marginal realism. This indicates that strict single-metric selection can be systematically misleading even under a small and practically relevant MSE tolerance.

We further test whether this pattern is an artifact of the candidate model pool. In Appendix B.1, we repeat the same 5% tolerance-band analysis using a broader set of forecasting models, including Linear, MLP, LSTM, N-BEATS, PatchTST, and TCN point forecasters, together with probabilistic variants. The same qualitative opportunity-cost pattern remains: near-tied alternatives within the MSE band continue to yield non-trivial marginal-realism gains across the

Dataset	REC_P	MIMO_P	f-REC <sub>s</sub>	f-MIMO <sub>s</sub>	f-REC <sub>m</sub>	f-MIMO <sub>m</sub>	Dataset	REC_P	MIMO_P	f-REC <sub>s</sub>	f-MIMO <sub>s</sub>	f-REC <sub>m</sub>	f-MIMO <sub>m</sub>
MG	0.42	0.44	0.0	0.0	0.1	0.02	MG	0.12	0.15	0.22	0.49	0.0	0.0
Electricity	0.17	0.4	0.0	0.0	0.0	0.42	Electricity	0.01	0.1	0.02	0.77	0.0	0.09
ExchangeRate	0.38	0.28	0.0	0.0	0.0	0.34	ExchangeRate	0.57	0.2	0.0	0.16	0.0	0.08
Weather	0.38	0.29	0.0	0.0	0.0	0.34	Weather	0.92	0.04	0.0	0.0	0.0	0.04
METR-LA	0.19	0.76	0.0	0.0	0.0	0.04	METR-LA	0.7	0.0	0.0	0.29	0.0	0.0
PEMS-BAY	0.01	0.93	0.0	0.0	0.0	0.06	PEMS-BAY	0.5	0.01	0.01	0.48	0.0	0.0
PEMS04	0.01	0.85	0.0	0.0	0.0	0.14	PEMS04	0.17	0.01	0.0	0.81	0.0	0.0
ETTh1	0.09	0.52	0.0	0.0	0.0	0.39	ETTh1	0.14	0.06	0.01	0.76	0.0	0.0
PEMS08	0.01	0.98	0.0	0.0	0.0	0.01	PEMS08	0.13	0.0	0.0	0.86	0.0	0.01
BeijingAirQuality	0.2	0.59	0.0	0.0	0.0	0.15	BeijingAirQuality	0.68	0.04	0.04	0.23	0.0	0.0
Average	0.19	0.6	0.0	0.0	0.01	0.19	Average	0.39	0.06	0.03	0.49	0.0	0.02

(a) Fraction of optimal selections under MSE loss.

(b) Fraction of optimal selections under  $W_1$  marginal loss.

**Table 1: Comparison of REC and MIMO strategies on real-world datasets. Values indicate the frequency with which each method is optimal for the respective metric (a) for mse and (b) for marginal realism. Subscripts  $s$  and  $m$  correspond to sample-based and mean-based flows; “-P” denotes point methods and “f-” denotes generative methods.**

evaluated datasets. Thus, the observed effect is not specific to the simpler candidate families used in the main sweep.

For probabilistic forecasts, we also examine whether improved marginal realism is merely obtained by producing wider, less informative predictive distributions. Appendix B.2 reports calibration and interval-width diagnostics for the best-realism candidate inside the same MSE tolerance band. These diagnostics show heterogeneous behavior rather than a uniform widening effect, so marginal realism, calibration, and sharpness should be treated as complementary model-selection criteria rather than interchangeable objectives.

**The uncertainty gap is not required for selection.** In synthetic systems, repeated rollouts allow us to estimate the conditional uncertainty gap directly and relate it to the geometry of the Pareto frontier. In real-world datasets, however, the conditional distribution  $p(Y_h | X)$  is not directly observable, so gap estimation is necessarily approximate.

Crucially, the practical opportunity-cost analysis does not require estimating the uncertainty gap. It is computed directly from quantities available under standard validation: candidate-model predictions, ground-truth futures, MSE, and empirical realism metrics. The gap explains why an accuracy–realism frontier should emerge under conditional uncertainty, but the tolerance-band selection statistic itself remains well-defined even when the gap is unknown or imperfectly estimated.

## 4.5 Strategies at MSE and Realism Extremes

While previous sections examined the geometry of the attainable accuracy–realism frontier, we now ask which forecasting strategies tend to occupy its *extremes*. Specifically, we analyze how different strategy and inference choices populate the MSE-optimal and realism-optimal ends across the 12,600 Pareto fronts attained (9 datasets  $\times$  7 variates  $\times$  200 horizons).

For each experimental configuration, we extract the Pareto front in the  $(\text{MSE}, W_1)$  plane and identify its two extreme members: the model with lowest MSE and the model with lowest marginal  $W_1$ . We then record the forecasting strategy associated with each extreme and compute the proportion of times each strategy occupies these positions across all experiments. Table 1 reports these membership ratios, grouped by dataset and averaged across domains.

The results reveal a strong and systematic clustering of Pareto extremes by strategy and inference choice. At the MSE-optimal extreme, direct MIMO point predictors dominate, accounting for 60% of lowest-MSE solutions on average, followed by MIMO probabilistic models using mean-based inference (19%). Notably, MIMO probabilistic models using single-sample inference never attain the MSE-optimal position in any experiment.

In contrast, the realism-optimal extreme is dominated by strategies that propagate or inject variability. Recursive point predictors account for 39% of lowest- $W_1$  solutions on average, while MIMO probabilistic models using single-sample inference account for 49%.

These patterns indicate that the extremes of the accuracy–realism frontier are instead strongly determined by the choice of inference mechanism. Direct or expectation-aligned inference consistently occupies the accuracy-optimal pole, while recursive and sample-based inference concentrate near the realism-optimal pole. This separation reinforces the view that strategy and inference choices act as mechanisms for navigating a multi-objective forecasting space, rather than simply improving performance along a single axis.

## 4.6 Practical Recommendation

Our results do not argue against MSE. Pointwise accuracy is often the primary operational constraint. The problem is stricter: under conditional uncertainty, models that are effectively tied in MSE can differ substantially in whether they reproduce the marginal variability of realized futures.

We therefore recommend a tolerance-band selection rule. First, identify the MSE-optimal model on validation data. Second, retain all candidates whose MSE lies within an application-dependent tolerance  $\epsilon$  of this optimum. Third, choose among these near-ties using marginal realism, measured here by  $W_1$ , as a simple diagnostic for dispersion. For probabilistic forecasts, this realism check should be paired with calibration and sharpness diagnostics, rejecting candidates with clearly worse coverage or unnecessarily wider predictive intervals.

The tolerance  $\epsilon$  encodes the downstream cost of sacrificing point accuracy. When small MSE differences are operationally decisive,  $\epsilon$  should be close to zero. When forecasts are used for simulation,

scenario generation, planning, stress testing, or long-horizon decision support, modest accuracy losses may be acceptable if they yield futures that better reflect realized variability. In our real-world experiments, even a 5% MSE band often exposes substantially more realistic alternatives.

Thus, marginal realism should not be optimized in isolation, nor should it replace proper probabilistic evaluation. Its role is more modest and practical: keep MSE as the primary constraint, then use inexpensive distributional diagnostics such as marginal  $W_1$ , together with calibration and sharpness where available, to select among models that are effectively tied under pointwise error.

## 5 Related Work

**Multi-step forecasting strategies.** Classical approaches to multi-step forecasting distinguish between recursive (iterated) and direct strategies, and analyze this choice primarily through a bias-variance trade-off under squared error loss [7–9, 28]. Early theoretical work showed that an oracle one-step predictor is generally biased for multi-step objectives [28]. More recent analyses, however, indicate that task bias does not necessarily translate into model bias in finite-sample regimes [7]. Existing empirical comparisons typically rank strategies using mean squared error (MSE), implicitly treating the conditional mean as the sole prediction target [9]. As a result, little attention has been paid to how different strategies affect the distributional properties of predicted trajectories or the variability of long-horizon forecasts.

**Forecasting benchmarks and evaluation protocols.** Recent benchmarks for time series forecasting remain heavily centered on pointwise error metrics such as MSE or MAE [10, 14, 20, 25, 26, 31]. However, this paradigm does not consider potential trade-offs between pointwise accuracy and distributional realism, nor does it examine whether near-optimal models under MSE may differ substantially in their distributional behavior.

**Distributional forecasting approaches.** Parallel work on probabilistic forecasting, popularized by DeepAR [24], emphasizes estimating predictive distributions rather than single point forecasts, and is commonly evaluated using proper scoring rules such as the CRPS [6, 11]. The ProbTS benchmark [32] explicitly evaluates both point and distributional forecasting across horizons, highlighting tensions between short-term probabilistic accuracy and long-term point accuracy. Related approaches include quantile forecasting [15], conformal prediction methods that construct prediction intervals with coverage guarantees [22], and generative models such as diffusion-based forecasters [21]. These methods are often presented as alternatives to point forecasting, with the ability to model predictive distributions viewed as a way to mitigate over-smoothing or uncertainty miscalibration.

In contrast, we show that the tension between pointwise accuracy and distributional realism arises from the conditional distribution itself. Once a decision rule is applied—such as reporting the predictive mean, median, or a sampled trajectory—these methods correspond to different operating points along the same accuracy-realism frontier, rather than eliminating the underlying trade-off.

**Expectation versus typical realizations.** The mismatch between conditional expectations and representative realizations is

well known in other areas of machine learning, particularly in generative modeling, where minimizing squared error can lead to mode averaging and visually unrealistic samples [17]. In such settings, the conditional mean is often not a meaningful output, and research has therefore shifted toward distributional or perceptual objectives that prioritize realistic samples over pointwise accuracy [29].

In contrast, time-series forecasting has historically remained centered on pointwise error metrics, with the conditional expectation treated as the canonical prediction target [13]. We instead show that, under nonzero conditional uncertainty, the mismatch between expectations and typical realizations is structurally unavoidable for deterministic predictors evaluated under squared loss, reframing oversmoothing as an intrinsic property of the forecasting objective rather than a limitation of model capacity or training.

**Positioning of this work.** In contrast to prior studies, which treat pointwise and distributional evaluation as separate modeling choices, we show that their incompatibility arises from a structural property of the conditional distribution itself. While multi-objective work has explored trade-offs between accuracy and practical costs [5, 19], it typically assumes only the MSE notion of accuracy. We instead show that, when conditional uncertainty is nonzero, no deterministic predictor can simultaneously minimize MSE and match the marginal distribution of realized futures, establishing an intrinsic trade-off between point accuracy and distributional realism.

## 6 Discussion and future work

**The practical cost of MSE-only evaluation.** Across nine real-world benchmarks, allowing a modest 5% relaxation in MSE yields a median improvement of 17.3% in marginal realism. This indicates that strict MSE-only model selection can systematically discard substantially more realistic forecasts, even when accuracy differences are small. This effect is not a corner case: every dataset exhibits regimes in which near-MSE-optimal models provide materially improved marginal distributional behavior. Together with our theoretical results, this suggests that single-metric evaluation can be structurally misleading in long-horizon forecasting.

**Strategy and inference as functional selection.** Recursive and direct strategies are traditionally compared through bias and variance analyses under squared loss. Our results suggest a more general interpretation: strategy and inference choices implicitly select which functional of the conditional future distribution is emphasized. Direct multi-output strategies and mean-based inference align with conditional expectations and therefore concentrate near the MSE-optimal extreme. Recursive strategies and sample-based inference propagate variability and more often occupy realism-favoring regions of the frontier. This perspective helps explain why empirical dominance between strategies is inconsistent across horizons and datasets [9]: they are not optimizing the same single objective [28], but navigating different regions of a multi-objective forecasting space.

**Implications for benchmarking and evaluation.** Current forecasting benchmarks predominantly rank methods using pointwise error metrics such as MSE or MAE. Our results indicate that this practice can obscure meaningful differences in distributional behavior at long horizons. A simple practical adjustment is to complement pointwise metrics with a distributional realism metric or

to evaluate models within a small MSE tolerance band and compare attainable realism gains. More broadly, we advocate reporting accuracy–realism trade-offs—such as using Pareto fronts in forecasting model selection [3] or dominance relations—rather than collapsing performance into a single scalar metric.

*Limitations and future directions.* Our main theoretical result is stated for deterministic predictors and deterministic inference rules. While probabilistic models can be embedded into this framework through specific decision rules, a full characterization of the accuracy–realism frontier for stochastic predictors remains open. Our notion of realism is also intentionally limited. Marginal  $W_1$  captures a simple and observable failure mode of MSE-optimal forecasting: under-dispersion across realized futures. It should not be interpreted as a sufficient condition for conditional correctness, calibration, or trajectory-level realism. In probabilistic forecasting settings, marginal realism should therefore be used alongside proper scoring rules, calibration diagnostics, and sharpness measures. Extending the analysis to trajectory-level objectives and nonstationary settings, such as concept drift, is a natural direction for future work.

## 6.1 Conclusion

We showed that when conditional uncertainty is nonzero, no deterministic predictor can simultaneously minimize mean squared error and match the marginal distribution of realized futures. This induces a fundamental accuracy–realism trade-off in multi-step forecasting. Empirically, across nine real-world benchmarks, a 5% tolerance in MSE yields a median 17.3% gain in marginal realism, demonstrating a tangible opportunity cost to strict MSE-only model selection. Our findings suggest that long-horizon forecasting performance is better understood as navigating an intrinsic accuracy–realism frontier rather than optimizing a single pointwise error metric. The practical implication is not to discard MSE, but to treat long-horizon forecasting under conditional uncertainty as a constrained multi-objective selection problem: keep MSE as the primary constraint, define an application-dependent tolerance band around the MSE optimum, and use inexpensive distributional diagnostics such as marginal  $W_1$ , together with calibration and sharpness checks where available, to choose among near-tied candidates.

## References

- [1] Abdul Fatir Ansari, Lorenzo Stella, Caner Turkmen, Xiyuan Zhang, Pedro Mercado, Huibin Shen, Oleksandr Shchur, Syama Sundar Rangapuram, Sebastian Pineda Arango, Shubham Kapoor, et al. 2024. Chronos: Learning the language of time series. *arXiv preprint arXiv:2403.07815* (2024).
- [2] Gianluca Bontempi, Souhaib Ben Taieb, and Yann-Aël Le Borgne. 2012. Machine learning strategies for time series forecasting. In *European Big Data Management and Analytics Summer School*. Springer, 62–77.
- [3] Oliver Borchert, David Salinas, Valentin Flunkert, Tim Januschowski, and Stephan Günnemann. 2022. Multi-objective model selection for time series forecasting. *arXiv preprint arXiv:2202.08485* (2022).
- [4] Laurent Dinh, Jascha Sohl-Dickstein, and Samy Bengio. 2016. Density estimation using real nvp. *arXiv preprint arXiv:1605.08803* (2016).
- [5] Raphael Fischer and Amal Saadallah. 2024. AutoXPCR: Automated multi-objective model selection for time series forecasting. In *Proceedings of the 30th ACM SIGKDD Conference on Knowledge Discovery and Data Mining*, 806–815.
- [6] Tilmann Gneiting and Adrian E Raftery. 2007. Strictly proper scoring rules, prediction, and estimation. *Journal of the American statistical Association* 102, 477 (2007), 359–378.
- [7] Riku Green, Huw Day, Zahraa S Abdallah, et al. 2025. Epistemic Error Decomposition for Multi-step Time Series Forecasting: Rethinking Bias-Variance in Recursive and Direct Strategies. *arXiv preprint arXiv:2511.11461* (2025).
- [8] Riku Green, Grant Stevens, Zahraa Abdallah, et al. 2024. Time-series classification for dynamic strategies in multi-step forecasting. *arXiv preprint arXiv:2402.08373* (2024).
- [9] Riku Green, Grant Stevens, Zahraa S Abdallah, and Telmo M Silva Filho. 2025. Stratify: unifying multi-step forecasting strategies: R. Green et al. *Data Mining and Knowledge Discovery* 39, 5 (2025), 64.
- [10] Yifan Hu, Yuante Li, Peiyuan Liu, Yuxia Zhu, Naiqi Li, Tao Dai, Shu-tao Xia, Dawei Cheng, and Changjun Jiang. 2025. Fintsb: A comprehensive and practical benchmark for financial time series forecasting. *arXiv preprint arXiv:2502.18834* (2025).
- [11] Alexander Jordan, Fabian Krüger, and Sebastian Lerch. 2019. Evaluating probabilistic forecasts with scoringRules. *Journal of Statistical Software* 90 (2019), 1–37.
- [12] Xiangjie Kong, Zhenghao Chen, Weiyao Liu, Kaili Ning, Lechao Zhang, Syaueq Muhammad Marier, Yichen Liu, Yuhao Chen, and Feng Xia. 2025. Deep learning for time series forecasting: a survey. *International Journal of Machine Learning and Cybernetics* (2025), 1–34.
- [13] Vincent Le Guen and Nicolas Thome. 2020. Probabilistic time series forecasting with shape and temporal diversity. *Advances in neural information processing systems* 33 (2020), 4427–4440.
- [14] Zhe Li, Xiangfei Qiu, Peng Chen, Yihang Wang, Hanyin Cheng, Yang Shu, Jilin Hu, Chenjuan Guo, Aoying Zhou, Christian S Jensen, et al. 2025. Tsfm-bench: A comprehensive and unified benchmark of foundation models for time series forecasting. In *Proceedings of the 31st ACM SIGKDD Conference on Knowledge Discovery and Data Mining V. 2*. 5595–5606.
- [15] Bryan Lim, Sercan Ö Arık, Nicolas Loeff, and Tomas Pfister. 2021. Temporal fusion transformers for interpretable multi-horizon time series forecasting. *International journal of forecasting* 37, 4 (2021), 1748–1764.
- [16] Michael C Mackey and Leon Glass. 1977. Oscillation and chaos in physiological control systems. *Science* 197, 4300 (1977), 287–289.
- [17] Luke Metz, Ben Poole, David Pfau, and Jascha Sohl-Dickstein. 2016. Unrolled generative adversarial networks. *arXiv preprint arXiv:1611.02163* (2016).
- [18] Kaisa Miettinen. 1999. *Nonlinear Multiobjective Optimization*. Springer.
- [19] Aviv Navon, Aviv Shamsian, Ethan Fetaya, and Gal Chechik. 2021. Learning the Pareto Front with HyperNetworks. In *International Conference on Learning Representations*.
- [20] Xiangfei Qiu, Jilin Hu, Lekui Zhou, Xingjian Wu, Junyang Du, Buang Zhang, Chenjuan Guo, Aoying Zhou, Christian S Jensen, Zhenli Sheng, et al. 2024. Tfb: Towards comprehensive and fair benchmarking of time series forecasting methods. *arXiv preprint arXiv:2403.20150* (2024).
- [21] Mohammad A. Rasul, Sheheryar Zaidi, Shirzad K. Hadrian, Tim Januschowski, and Stephan Günnemann. 2021. TimeGrad: Autoregressive Denoising Diffusion Models for Multivariate Probabilistic Time Series Forecasting. *arXiv preprint arXiv:2106.16214* (2021).
- [22] Yaniv Romano, Evan Patterson, and Emmanuel Candes. 2019. Conformalized quantile regression. *Advances in neural information processing systems* 32 (2019).
- [23] Hiroaki Sakoe and Seibi Chiba. 1978. Dynamic Programming Algorithm Optimization for Spoken Word Recognition. *IEEE Transactions on Acoustics, Speech, and Signal Processing* 26, 1 (1978), 43–49. doi:10.1109/TASSP.1978.1163055
- [24] David Salinas, Valentin Flunkert, and Jan Gasthaus. 2017. DeepAR: Probabilistic Forecasting with Autoregressive Recurrent Networks. *arXiv preprint arXiv:1704.04110* (2017).
- [25] Zezhi Shao, Fei Wang, Yongjun Xu, Wei Wei, Chengqing Yu, Zhao Zhang, Di Yao, Tao Sun, Guangyin Jin, Xin Cao, et al. 2024. Exploring progress in multivariate time series forecasting: Comprehensive benchmarking and heterogeneity analysis. *IEEE Transactions on Knowledge and Data Engineering* (2024).
- [26] Eivind Strøm and Odd Erik Gundersen. 2024. Performance metrics for multi-step forecasting measuring win-loss, seasonal variance and forecast stability: an empirical study. *Applied Intelligence* 54, 21 (2024), 10490–10515.
- [27] Bing Su and Gang Hua. 2017. Order-preserving wasserstein distance for sequence matching. In *Proceedings of the IEEE conference on computer vision and pattern recognition*. 1049–1057.
- [28] Souhaib Ben Taieb. 2014. Machine learning strategies for multi-step-ahead time series forecasting. *Universit Libre de Bruxelles, Belgium* (2014), 75–86.
- [29] Lucas Theis, Aaron van den Oord, and Matthias Bethge. 2015. A note on the evaluation of generative models. *arXiv preprint arXiv:1511.01844* (2015).
- [30] Titouan Vayer, Laetitia Chapel, Rémi Flamary, Romain Tavenard, and Nicolas Courty. 2020. Fused Gromov-Wasserstein distance for structured objects. *Algorithms* 13, 9 (2020), 212.
- [31] Yuxuan Wang, Haixu Wu, Jiayang Dong, Yong Liu, Chen Wang, Mingsheng Long, and Jianmin Wang. 2024. Deep time series models: A comprehensive survey and benchmark. *arXiv preprint arXiv:2407.13278* (2024).
- [32] Jiawen Zhang, Xumeng Wen, Zhenwei Zhang, Shun Zheng, Jia Li, and Jiang Bian. 2024. ProTBS: Benchmarking point and distributional forecasting across diverse prediction horizons. *Advances in Neural Information Processing Systems* 37 (2024), 48045–48082.

## A Dataset and Experimental Details

### A.1 Real-world benchmarks

We use the nine real-world datasets from [25]: ETTh1 ( $T=14,400$ ), Electricity ( $T=26,304$ ), METR-LA ( $T=34,272$ ), PEMS04 ( $T=16,992$ ), PEMS08 ( $T=17,856$ ), PEMS-BAY ( $T=52,116$ ), Weather ( $T=52,696$ ), BeijingAirQuality ( $T=36,000$ ), and ExchangeRate ( $T=7,588$ ). For each dataset, we treat the first seven variates as separate univariate forecasting tasks.

Each series is split chronologically, with the first 80% used for training and the remaining 20% for evaluation. All experiments use a lag window of length  $L = 20$  and a forecast horizon of  $H = 200$ . We draw  $N_{\text{eval}} = 1000$  evaluation windows uniformly from the test portion of each series. Each univariate series is standardized using the training-set mean and standard deviation, and all reported metrics are computed in this normalized space.

### A.2 Forecasting models and inference rules

The main empirical sweep evaluates deterministic point forecasters under recursive (REC) and direct multi-output (MIMO) strategies using Linear Ridge Regression, MLPs, and Decision Trees. We additionally train conditional normalizing flows under both REC and MIMO formulations and evaluate them using deterministic inference rules such as predictive means and single-sample rollouts. All models are trained with fixed hyperparameters and without dataset-specific tuning: Ridge uses  $\alpha = 0.1$ , MLPs use one 2048-unit hidden layer with  $\alpha \in \{0, 8\}$ , decision trees use maximum depth 10, and RealNVP flows use 12 affine coupling layers with hidden widths  $\{16, 64, 256\}$ . The purpose of the model set is to sample attainable operating points on the accuracy–realism frontier rather than to exhaustively optimize each benchmark.

### A.3 Synthetic Mackey–Glass setting

For the controlled experiments in Section 4.1, we generate data from a stochastic Mackey–Glass system with additive state noise of magnitude  $\sigma_s$ , using the standard delayed-feedback recursion from [16]. Unless otherwise stated, we use  $a = 0.1$ ,  $\gamma = 0.2$ ,  $\tau = 17$ , a burn-in of 100 steps, total length  $T = 6000$ , lag  $L = 20$ , horizon  $H = 200$ , and an 80/20 chronological split. For each selected test context, we approximate the conditional distribution using 1000 Monte Carlo rollouts

### A.4 Auxiliary realism metrics

Our primary realism metric is marginal  $W_1$ , because it is hyperparameter free, horizon-local, and directly targets the underdispersion mechanism central to the paper. As complementary structural checks, we also report Dynamic Time Warping (DTW) [23], vector Wasserstein distance, order-preserving Wasserstein (OPW) [27], and fused Gromov–Wasserstein (FGW) [30]. These trajectory-level metrics emphasize different aspects of temporal alignment, value distribution, and geometric structure. We omit full equations here for space; our main empirical claims are in terms of marginal  $W_1$ .

We do not rely on real-world estimates of the conditional uncertainty gap in the final model-selection analysis. Any finite-sample proxy for the gap mixes the underlying signal with estimator bias

Dataset	Mean	Med.	IQR	Gain > 5
ExchangeRate	21.7	11.7	[3.9, 33.5]	70.9
PEMS08	15.1	12.5	[5.9, 20.8]	77.5
Weather	12.5	8.8	[3.2, 16.1]	67.3
ETTh1	18.5	17.1	[7.8, 27.5]	83.2
MG	15.5	13.2	[9.4, 18.0]	94.1

**Table 2: Robustness of the 5% MSE tolerance-band analysis under a stronger candidate model set. Mean, median, and IQR denote relative marginal-realism gains (%) for the best-realism model inside the 5% MSE band compared with the MSE-optimal model. Gain > 5 denotes the percentage of cases in which the realism gain exceeds 5%.**

and variance, so we treat such quantities as explanatory diagnostics rather than deployment-time requirements.

## B Additional Robustness Checks

### B.1 Stronger candidate model set

To test whether the tolerance-band effect persists under a broader candidate pool, we repeat the same 5% MSE tolerance-band analysis using an expanded set of forecasting models. The point-forecasting pool includes Linear, MLP, LSTM, N-BEATS, PatchTST, and TCN models. The probabilistic pool includes Linear, MLP, LSTM, normalizing flow, PatchTST, and TCN variants.

For each horizon-specific evaluation, we identify the MSE optimal candidate and then select the candidate with the best marginal realism among all models whose MSE lies within 5% of this optimum. Table 2 reports the relative marginal-realism gain of this near-MSE-optimal alternative, together with the percentage of cases in which the realism gain exceeds 5%.

The opportunity-cost pattern remains visible under the expanded model set. Median marginal-realism gains are non-trivial across all evaluated datasets, and the proportion of cases with realism gain above 5% ranges from 67.3% to 94.1%. This indicates that the practical effect identified in the main text is not specific to the simpler model families used in the main sweep.

### B.2 Probabilistic forecasts: calibration and width

Marginal realism alone does not determine whether a probabilistic forecast is conditionally well calibrated. A model could improve marginal distributional agreement by producing less informative wider predictive distributions. We complement the marginal-realism analysis with coverage and interval-width diagnostics.

For each horizon-specific evaluation, we again consider the best-realism candidate inside the 5% MSE band and compare it with the MSE-optimal candidate. Table 3 reports the median realism gain, the change in empirical 80% coverage, and the change in predictive interval width. Positive  $\Delta C_{80}$  indicates improved agreement with nominal 80% coverage. Positive  $\Delta I$  indicates wider intervals and hence lower sharpness.

The relation between marginal realism, calibration, and width is heterogeneous. The realism-selected candidate is not typically

Dataset	Med. $\Delta R$	Mean $\Delta C_{80}$	Med. $\Delta C_{80}$	Mean $\Delta I$	Med. $\Delta I$
ExchangeRate	23.1	1.306	0.000	14.3	26.3
PEMS08	13.5	0.308	0.000	-2.9	-1.2
Weather	9.6	0.209	0.017	-0.03	-0.00
ETTh1	13.7	0.727	0.264	2.4	0.0
MG	13.1	0.401	0.000	-1.8	0.0

**Table 3: Calibration and interval-width diagnostics for the best-realism probabilistic forecast inside the 5% MSE band compared with the MSE-optimal forecast.  $\Delta R$  is the relative marginal-realism gain (%). Positive  $\Delta C_{80}$  indicates improved empirical 80% coverage.  $\Delta I$  is the relative change in predictive interval width (%); positive values indicate wider and hence less sharp intervals.**

Metric	$\widetilde{\Delta R}$	$IQR(\Delta R)$	$\widetilde{p}_{hit}$	$IQR(p_{hit})$
$W_1$	0.17	[0.10, 0.28]	0.31	[0.25, 0.32]
DTW	0.07	[0.06, 0.10]	0.10	[0.08, 0.12]
$W_1\text{-vec}$	0.08	[0.06, 0.10]	0.15	[0.11, 0.16]
OPW	0.09	[0.07, 0.12]	0.04	[0.01, 0.10]
FGW	0.11	[0.07, 0.17]	0.19	[0.16, 0.23]

**Table 4: Multi-metric opportunity cost under an MSE tolerance of  $\epsilon = 5\%$ . For each realism metric, we report the median across datasets of the dataset-level median realism gain ( $\widetilde{\Delta R}$ ) and the dataset-level hit rate ( $\widetilde{p}_{hit}$ ), together with the corresponding interquartile ranges across datasets. ‘‘Hit’’ denotes  $\Delta Realism > \Delta MSE$ .**

worse under the 80% coverage diagnostic, and realism gains are not uniformly obtained by widening predictive intervals. ExchangeRate shows a clear increase in width, whereas PEMS08, Weather, and MG exhibit zero or negative median width changes while still obtaining non-trivial realism gains. This rules out the simplest universal explanation that realism gains are always purchased through indiscriminate over-dispersion.

### B.3 Robustness across alternative realism metrics

Table 4 reports the same  $\epsilon=5\%$  opportunity-cost analysis under multiple notions of realism. For each dataset, variate, and horizon-specific evaluation, we identify the MSE-optimal model and then consider Pareto-optimal alternatives whose MSE is within  $(1 + \epsilon)\%$  of the optimum. Within this near-tie set, we record the best attainable improvement in realism for a given metric and the hit rate  $\Delta Realism > \Delta MSE$ .

The opportunity-cost effect remains visible beyond marginal  $W_1$ , but its magnitude depends strongly on the realism notion used. Marginal  $W_1$  yields the largest gains and highest hit rates because it targets the horizon-wise dispersion mismatch central to our theory, whereas trajectory metrics impose stronger structural correspondence and thus typically require larger departures from the MSE optimum.

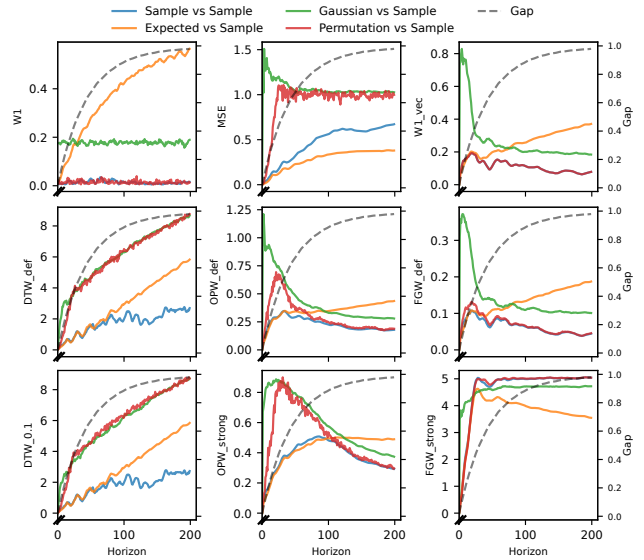


**Figure 7: Metric audit on the stochastic Mackey–Glass system. We compare four deterministic sequences against an independent DGP sample: sample vs sample, conditional expectation vs sample, variance matched Gaussian vs sample, and permutation vs sample. The diagnostic asks whether a metric (i) keeps sample-vs-sample small, (ii) makes expectation-vs-sample grow with uncertainty, and (iii) penalizes permutations when temporal structure is broken. Marginal  $W_1$  satisfies (i) and (ii) cleanly, but not (iii), since it ignores order. DTW, OPW, FGW, and  $W_1\text{-vec}$  are more sensitive to temporal structure, but also respond more strongly to alignment and point-wise deviations.**

### B.4 What different realism metrics detect

A useful realism metric should reflect the kind of mismatch one aims to detect. In our setting, the primary failure mode is *under-dispersion*: the MSE-optimal conditional expectation can be accurate on average while becoming unrepresentative of typical realized futures. Under a single-realization evaluation protocol, this suggests three desiderata for a diagnostic metric. First, two independent samples from the same data-generating process should be judged similar. Second, the conditional expectation should move further away from a realized sample as conditional uncertainty grows. Third, if temporal structure is part of the realism notion, then a sample should be distinguishable from a within-trajectory permutation of itself.

Figure 7 shows that marginal  $W_1$  is the clearest diagnostic for the phenomenon studied here. It keeps sample-vs-sample near zero while making expectation-vs-sample grow with uncertainty, directly exposing the under-dispersion of the conditional mean. Its limitation is that permutation-vs-sample is also small, since marginal  $W_1$  ignores temporal order.

DTW, OPW, FGW, and  $W_1\text{-vec}$  attempt to encode stronger notions of trajectory similarity. However, this makes them more sensitive to ordering and shape distortions, but also more correlated with pointwise error, which helps explain their smaller opportunity-cost

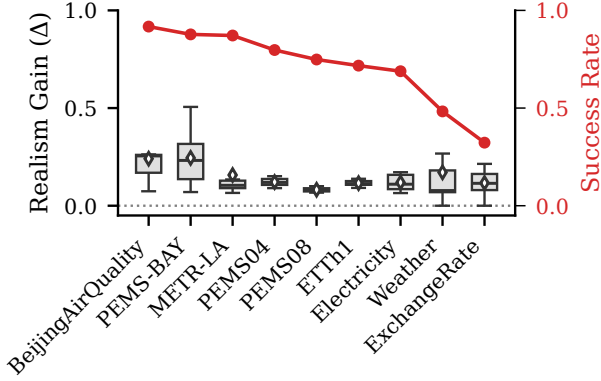


**Figure 8: Reproduction of the main-text  $\epsilon$ -opportunity summary using zero-shot Chronos-T5 (lookback 512,  $H \leq 50$ ), following the settings recommended in [1].**

gains. We therefore use marginal  $W_1$  as the paper’s primary realism axis and treat the trajectory metrics as complementary checks.

### B.5 Zero-shot Chronos robustness

As an additional robustness check using a strong forecasting foundation model, we evaluate Amazon Chronos-T5 [1] in zero-shot mode on the same real-world benchmarks. We use the same dataset splits as in the main experiments, standardize each series independently, and construct rolling forecasting instances with lookback 512 and horizons up to 50, following the operating range recommended by the Chronos authors.

We evaluate three Chronos sizes (chronos-t5-tiny, chronos-t5-mini, chronos-t5-small) across sampling temperatures  $\tau \in \{0.6, 0.8, 1.0, 1.2, 1.4\}$ . For each context we draw 100 forecast samples and form operating points using either individual sampled trajectories or means of multiple samples. As in the main paper, sample-based operating points occupy the realism-favored region, whereas mean-of-samples forecasts concentrate near the MSE-favored extreme.

The same  $\epsilon$ -opportunity pattern remains visible under Chronos. Across datasets we observe consistently positive median realism gains together with generally high hit rates. The strongest results are on BeijingAirQuality (0.92 hit rate; median/mean gain 0.25/0.24), PEMS-BAY (0.88; 0.23/0.24), and METR-LA (0.87; 0.10/0.16). We also observe positive median gains on PEMS04 (0.80; 0.12/0.12), PEMS08 (0.75; 0.08/0.08), ETTh1 (0.72; 0.11/0.12), Electricity (0.69; 0.11/0.12), Weather (0.48; 0.08/0.17), and ExchangeRate (0.32; 0.11/0.12). Thus, the practical opportunity cost of strict MSE-only selection is also visible for a strong zero-shot foundation model.

## C Additional Theoretical Results

This section records short extensions of Theorem 1.

### C.1 Why determinism matters

Theorem 1 is stated for deterministic point predictors, which is the standard setting for MSE-trained multi-step forecasters. The key fact is that stochastic randomization cannot improve expected MSE beyond the conditional mean.

**PROPOSITION 2 (RANDOMIZATION CANNOT IMPROVE MSE).** *Let  $\hat{Y}_h$  be any (possibly randomized) predictor given  $\mathbf{X}$  with finite second moment. Then*

$$\mathbb{E}\left[(\hat{Y}_h - Y_h)^2\right] \geq \mathbb{E}\left[(\mathbb{E}[Y_h | \mathbf{X}] - Y_h)^2\right],$$

with equality if and only if  $\hat{Y}_h = \mathbb{E}[Y_h | \mathbf{X}]$  almost surely.

*Proof sketch.* Conditioning on  $\mathbf{X}$  gives

$$\mathbb{E}\left[(\hat{Y}_h - Y_h)^2 | \mathbf{X}\right] = \mathbb{E}\left[(\hat{Y}_h - \mathbb{E}[Y_h | \mathbf{X}])^2 | \mathbf{X}\right] + \text{Var}(Y_h | \mathbf{X}),$$

where the cross-term vanishes. Taking expectation over  $\mathbf{X}$  yields the result. Thus, any stochasticity that helps match a distributional target must be paid for in expected MSE.

### C.2 Single-context trajectory mismatch

Theorem 1 compares marginal laws after averaging over contexts. A complementary statement holds at the level of conditional trajectory laws for a fixed context.

Let  $\mathbf{Y}_{:H} = (Y_1, \dots, Y_H) \in \mathbb{R}^H$  denote the future trajectory and define

$$P_x := \mathcal{L}(\mathbf{Y}_{:H} | \mathbf{X} = x), \quad \mathbf{m}(x) := \mathbb{E}[\mathbf{Y}_{:H} | \mathbf{X} = x].$$

The Bayes-optimal deterministic predictor under vector MSE is  $\mathbf{m}(x)$ . Because this predictor is deterministic, its conditional predictive law is the Dirac measure  $\delta_{\mathbf{m}(x)}$ .

**PROPOSITION 3 (CONDITIONAL TRAJECTORY MISMATCH).** *Assume  $\mathbb{E}\|\mathbf{Y}_{:H}\|^2 < \infty$ . Then for any fixed context  $x$ ,*

$$\begin{aligned} W_2^2(P_x, \delta_{\mathbf{m}(x)}) &= \mathbb{E}\left[\|\mathbf{Y}_{:H} - \mathbf{m}(x)\|^2 | \mathbf{X} = x\right] \\ &= \text{tr}(\text{Cov}(\mathbf{Y}_{:H} | \mathbf{X} = x)). \end{aligned}$$

*In particular, if  $\text{tr}(\text{Cov}(\mathbf{Y}_{:H} | \mathbf{X} = x)) > 0$ , then  $W_2(P_x, \delta_{\mathbf{m}(x)}) > 0$ .*

*Proof sketch.* The only coupling between  $P_x$  and a Dirac mass  $\delta_a$  pairs  $\mathbf{Y}_{:H}$  with the constant vector  $a$ , so  $W_2^2(P_x, \delta_a) = \mathbb{E}\left[\|\mathbf{Y}_{:H} - a\|^2 | \mathbf{X} = x\right]$ . Minimizing over  $a$  gives  $a = \mathbf{m}(x)$ , and the result follows from the standard identity between expected squared deviation and the trace of the conditional covariance matrix.

*Implication for trajectory-level law metrics.* Proposition 3 is stated with  $W_2$ , but the mismatch is not specific to Wasserstein distance. Whenever  $P_x$  is non-degenerate, we have  $P_x \neq \delta_{\mathbf{m}(x)}$ , so any trajectory-level metric or divergence on *probability laws over trajectories* that vanishes only when the two laws are equal must also be strictly positive at  $(P_x, \delta_{\mathbf{m}(x)})$ . Moreover, equality of trajectory laws implies equality of all horizon-wise marginals by coordinate projection; hence a mismatch at any marginal horizon already rules out any stronger trajectory-law match. This statement does not automatically extend to arbitrary instance-level sequence distances such as DTW between two sampled trajectories, which compare individual realizations rather than conditional laws.